Proc. Indian Acad. Sci. (*Chem. Sci.*), Vol. 115, Nos 5 & 6, October–December 2003, pp 525–532

Following the crystallisation of $Bi_2Mo_2O_9$ catalyst by combined XRD/QuEXAFS[¶]

ANDREW M BEALE and GOPINATHAN SANKAR*
Davy Faraday Research Laboratory, The Royal Institution of Great Britain,
21 Albemarle Street, London W1S 4BS, UK
e-mail: sankar@ri.ac.uk

Abstract. The formation of *b*-phase $Bi_2Mo_2O_9$ catalyst from a precursor precipitate has been studied using the *in situ* combined XRD/QuEXAFS technique and DSC during calcination. Accordingly the precursor was observed to undergo a number of changes in both the molybdenum (VI) coordination and long-range ordering during this heating. Initially the two other forms of bismuth molybdate (*a*- and *g*-phases) were observed to form from the poorly crystalline precursor at about 230°C, however, the *b*-phase eventually crystallised after prolonged heating at 560°C.

Keywords. $Bi_2Mo_2O_9$ catalyst; XRD/QuEXAFS; long-range.

1. Introduction

Bismuth molybdate materials having the general chemical formula $Bi_2O_3.nMoO_3$ (where $n = 3$, 2 or 1 and correspond to the *a*-, *b*- and *g*-phases respectively) are known to be excellent catalysts for the partial (amm) oxidation of light olefins[1,2]. Although compositionally very similar, they are structurally quite distinct with the *a*- and *b*-phases often described as possessing defect fluorite structures, whereas the *g*-phase is considered a classical example of an Auruvillius structure.[3–8] The coordination of both the bismuth (III) and molybdenum (VI) cations within these materials is also different with, for example, the *a*- and *b*-phases both containing BiO_8 units and MoO_4 tetrahedra (although in the former case the presence of a fifth oxygen at 2·29 Å is often considered as evidence that molybdenum is in 5-coordination geometry) whereas both environments in the *g*-phase are considered to be distorted six-coordination geometry.[3–9] Since the first patent dealing with the use of bismuth molybdate as catalysts,[10] several research articles and patents have appeared in the literature, many of which detail new preparative methods or catalyst formulation.[2,11–18] In general, these materials are formed via coprecipitation techniques[19] in which appropriate amounts of a bismuth source (normally bismuth nitrate) is dissolved in water, and to this is added a source of molybdenum ions in solution, normally through the dissolution of ammonium heptamolybdate. At this stage the pH is adjusted before the mix is aged, washed and dried to yield a precursor material, which is then calcined at elevated temperatures (between ≈400 and 700°C) to remove any volatilites and to form the final crystalline material; this method being preferred to the heating of a mixture of solid oxides since it is both quicker and allows for reactant mixing at the atomic level and thus avoids sample inhomogeneity problems. However,

[¶]Dedicated to Professor C N R Rao on his 70th birthday
*For correspondence

the preparation of stable, pure phase of these materials is often difficult to achieve, since the crystallisation of more than one phase occurs at these temperatures.[20]

Whilst there have been many studies to accurately determine both the structure of these phases and the origin of their catalytic behaviour, their production from the respective precursor is poorly understood. Recently we reported the results from an *in situ* study into the formation of the α- and γ-phases using hydrothermal methods[21]. However, we found it difficult to prepare the β-phase using such methods and hence we adopted the conventional precipitation method to prepare this highly catalytically active form of the bismuth molybdate family. Here we report an *in situ* XRD/QuEXAFS[22,23] study (supported by measurements carried out using DSC, SEM and XRD) of the formation of the β-phase from the precursor gel. The advantages in using the *in situ* XRD/QuEXAFS approach is that the technique allows us to compare changes in long- and short-range coordination during the activation process giving us an insight into the possible mechanism of formation; such an approach has previously been employed to understand the formation of the γ-phase from a precursor gel as well as for the study of phase transformations in other solid state systems.[22,24,25] Our investigation clearly showed that the poorly crystalline precursor material underwent a number of changes in both short- and long-range ordering before the final β-phase was observed to form fully when the calcination temperature reached 560°C.

2. Experimental

For the preparation of the bismuth molybdate precursor with the stoichiometry $Bi_2O_3.nMoO_3$ (where $n = 2$) we used similar procedures to those previously reported.[20] Stoichiometric amounts of acidified bismuth nitrate solution were mixed with ammonium heptamolybdate tetrahydrate dissolved in dilute ammonium hydroxide. The pH of the gel was adjusted to $\approx 4{\cdot}0$ before the excess water was boiled off and the pale yellow solid precursor was placed in an oven held at 100°C overnight to dry.

The XRD pattern of the as-synthesised material was recorded using Siemens D500 diffractometer (of Bragg–Brentano geometry) equipped with a copper target. DSC measurements were carried out using a Shimadzu DSC 50 with the samples heated in air at a rate of 10°C/minute from room temperature to 600°. Scanning electron micrograph (SEM) pictures were taken using a Jeol 733 Superprobe with an Oxford Instruments ISIS/INCA system for EDX analysis.

In situ XRD/QuEXAFS measurements were carried out at station 9·3 of Daresbury Synchrotron radiation source, which operates at 2 GeV with a typical current of 150 to 250 mA. The station was equipped with a Si(220) double crystal monochromator, and ion chambers for measuring incident and transmitted beam intensities for recording X-ray absorption spectra. For diffraction measurements, a position sensitive INEL detector was used. In a typical experiment, about 40 mg of the bismuth molybdate precursors were pressed in to a disc of 13 mm diameter. These samples were then placed into an *in situ* cell that permits the measurement of combined XAS and XRD data. The samples were heated at 5°C/min from room temperature to 560°C and this temperature was maintained for 120 min. Mo K-edge XAS and XRD data were collected sequentially, throughout this activation process. The time taken to record the Mo K-edge XAS pattern was 380 s and 180 s for XRD data resulting in a total cycle time of 10 min, which included 40 s dead-time to move the monochromator back to the starting point. XRD data were collected at a wavelength of 0·928 Å, (well below both the Mo K and Bi LIII-edges) to avoid

fluorescence effects. The INEL detector was calibrated using a NBS silicon standard and a 10 μm Mo foil was used to calibrate the monochromator position. XAS data were processed using the suite of programs available at Daresbury laboratory, namely EXCALIB (for converting the raw data to energy vs absorption coefficient) and EXBROOK to obtain the normalised XANES part of the spectra.

3. Results

First we discuss the results obtained from the XRD measurement of the dried precursor before we analyse the results obtained from the DSC and finally we follow the changes that took place during the calcination process using the *in situ* combined XRD/QuEXAFS technique.

In figure 1 we show the X-ray diffraction patterns of the dried precursor starting material and the final crystalline product of $Bi_2Mo_2O_9$. The pattern is dominated by a strong but very broad reflection at $\approx 28°2\theta$ along with additional reflections present at $\approx 24{\cdot}49$ and $46{\cdot}10°2\theta$. Although the presence of a reflection at $\approx 28°2\theta$ is a common feature in the XRD patterns for all three of the catalytically active forms of bismuth molybdate (as well as for MoO_3 and both the α- and β-forms of Bi_2O_3) none of these peaks can be indexed to any of these known phases.[26] This pattern may however, be due to the formation of a bismuth containing heteropolymolybdate that has been postulated to form under the conditions used here to prepare the precursor and are thought to be important for specific phase (particularly the α-phase) to form.[27]

In figure 2 is we show the DSC plot for the dried precursor during heating in air to 560°C. The plot contained a number of distinct exotherms at 60, 130, 170, 230 and

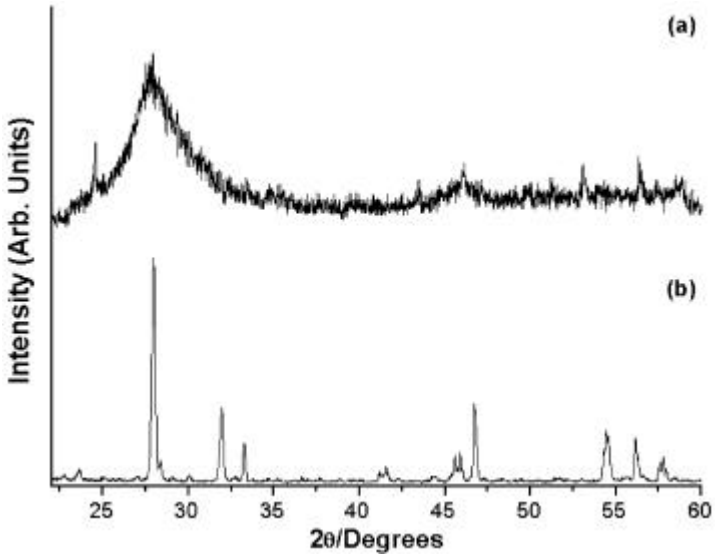

Figure 1. XRD patterns of (a) the β-precursor prepared by coprecipitation and after drying overnight in an oven at 100°C and (b) after calcination at 560°C for two hours.

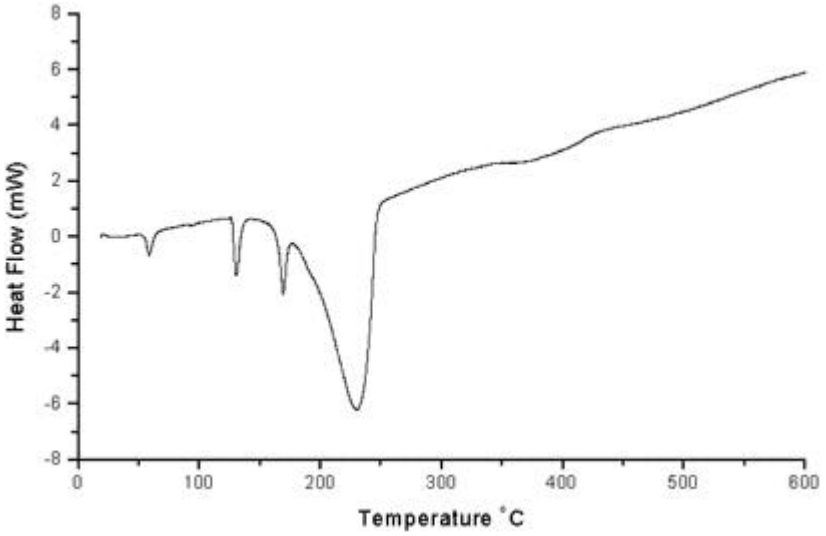

Figure 2. DSC trace recorded during the course of heating the *b*-precursor in air up to 560°C.

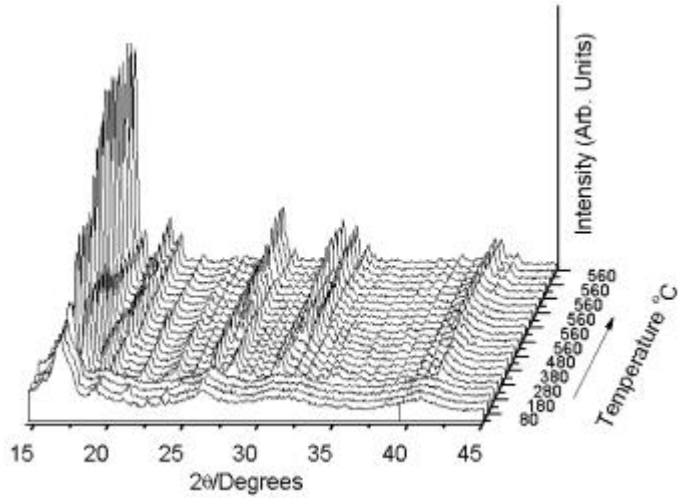

Figure 3. Stacked XRD plot obtained using the position sensitive INEL detector, during the course of heating the *b*-precursor, from room temperature to 560°C at a rate of 5°C per minute. XRD patterns were collected at a wavelength of 0·928 Å.

between 350–400°C. In figure 3 we show the stacked plot of the XRD data recorded, using the combined XRD/QuEXAFS for the ***b***-precursor during calcination in air to 560°C. It is clear that the XRD pattern shows number of changes during this process indicating that the poorly crystalline material is transformed in to crystalline systems. Initially, between 30 and 80°C, only small changes in some of the peak intensities present in the diffraction pattern of the original precursor were observed. On reaching tempe-

ratures in excess of 130°C some of the reflections present at 80°C, disappeared leaving (with the exception of the broad peak at ≈ 17°2θ), an essentially featureless pattern. A number of new reflections began to appear when the temperature is raised above 230°C, which can be readily identified as being due to the formation of the α and γ-phases. Beyond this temperature and up until the temperature reached 560°C only subtle changes in the XRD patterns were observed which involved an increase in peak intensity and decrease in peak width (FWHM). However after almost two hours of heating at this

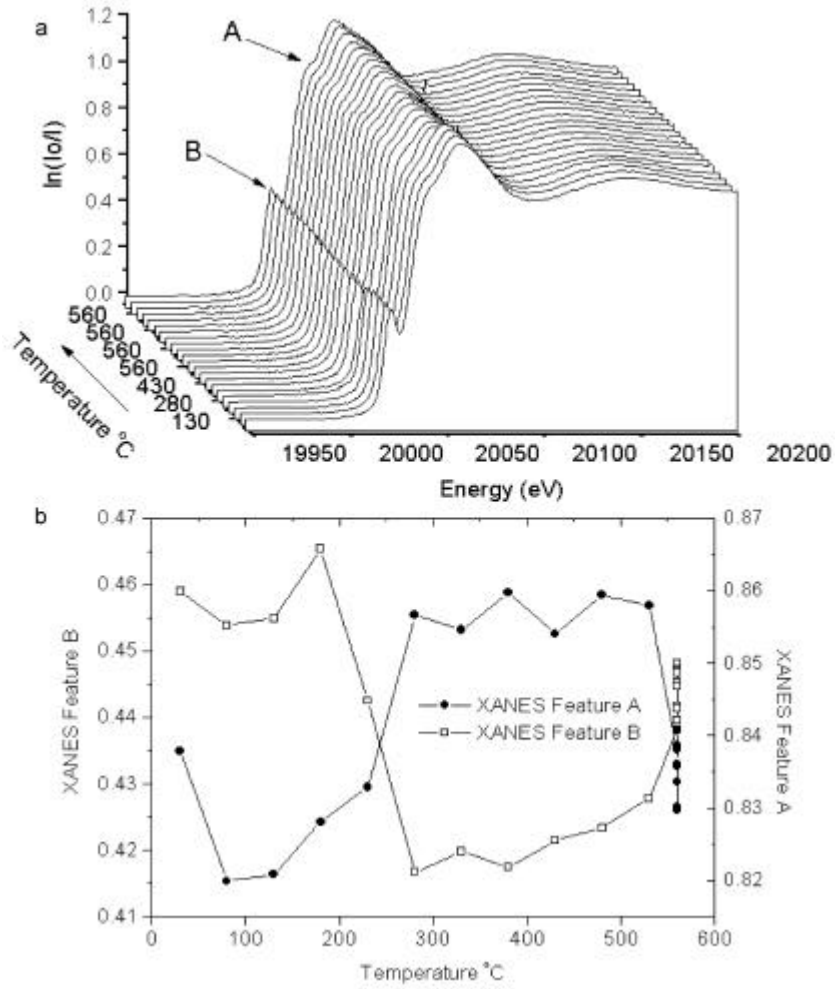

Figure 4. (**a**) Stacked Mo K-edge XANES data (for clarity we show only the small region, although the entire Mo K-edge XAS pattern was recorded within 380 s) recorded sequentially with the XRD pattern shown in figure 3. (**b**) Variation in the intensity of the features A and B with temperature. The main changes were seen to occur at temperatures above 230°C, which were due initially to the growth of a mixture of α- and γ-phases containing molybdenum in a higher coordination than the precursor. On reaching 560°C the decrease in intensity of the XANES feature marked A and increase in feature B heralded the appearance of the β-phase containing tetrahedral molybdenum.

temperature the reflections belonging to *α*- and *γ*-phases had disappeared with only reflections for the *β*-phase present in the XRD patterns.

Close inspection of the stacked Mo K-edge XANES data in figure 4a (recorded sequentially with the XRD data plotted in figure 3) clearly indicated that a change in some of the well-defined features of the spectrum had also taken place during calcination, suggesting that a change in the local coordination around molybdenum had occurred. Initially the XANES is dominated by the pre-edge feature marked in the figure as B which has previously been taken as evidence of Mo(VI) ions in a tetrahedral environment surrounded by four oxygens.[9,21,24] However on calcination above 230°C the decline in the intensity of this feature (figure 4b) and an increases in prominence of feature A coincided with the crystallisation of the *α*- and *γ*-phases which possess a higher coordination number. The features of the Mo K-edge XANES then remained unaltered until the calcination temperature reached 560°C at which point the intensity of feature A began to decline, whilst simultaneously, feature B began to grow. The SEM photograph of the sample obtained after heat treatment at 560°C for two hours is shown in figure 5. The sample appeared to be inhomogeneous and contained a number of particles possessing a variety of different shapes and sizes.

4. Discussion

The Mo K-edge XANES data for the *β*-precursor lead us to conclude that initially a four coordinated Mo(VI) containing material is formed and that this undergoes a number of changes during calcination to form the final *β*-phase material. In the early stages of heat treatment (< 250°C) the long-range ordering of this precursor material undergoes a number of changes as evidenced from the changes in the XRD patterns and a number of exotherms in the DSC trace. The largest of these exotherms (at ≈250°C) corresponds to the crystallisation of both the *α*- and *γ*-phase from the precursor with no sign of the *β*-

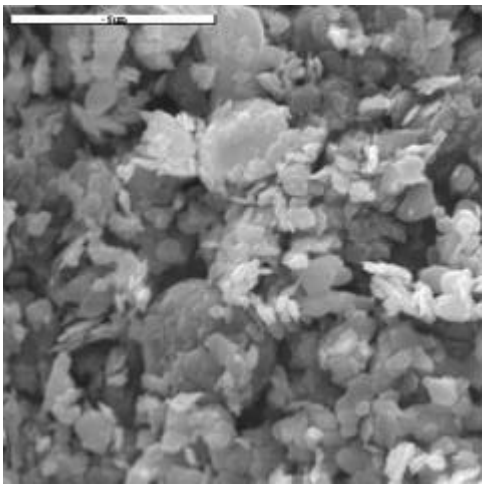

Figure 5. Scanning electron micrograph (SEM) images (magnified ×8000) of the *β*-phase formed after calcination of the respective precursors at 560°C. The white scale bar = 5 *μ*m.

phase observed until the calcination temperature reaches 560°C. The XRD results are consistent with the XANES observation that local coordination around Mo(IV) takes place corresponding to the formation of α- and γ-phases above 230°C. It appears, therefore, that the formation of this phase is via a solid-state reaction between the α- and γ-phases which are formed at the initial stages, as observed from changes in both the XRD and XANES data, after decomposition of the precursor at $\approx$ 250°C. Such observations are consistent with previous work in which it had been noted that this phase is very difficult to form using a copreciptation approach at low temperatures but that the phase does form readily from a solid mixture of the α- and γ-phases heated at high temperatures.[20,28] It may be that prolonged heating at high temperature, necessary to form this phase, results in the particle coalescence leading to the formation of a variety of particle shapes and sizes seen in the SEM image.

In summary, this study has shown clearly how the β-phase forms from a precursor that initially transforms to α- γ-phases of bismuth molybdate which reacts further, after prolonged heating at 560°C, to yield the final product. Furthermore this study has also demonstrated the need to employ either high temperatures or long calcination times to prepare this material since a failure to do so may result in a catalytically inferior or structurally unstable material.

Acknowledgements

The authors thank EPSRC for general financial support and CCLRC for synchrotron radiation beam time at Daresbury laboratory. We also thank the Leverhulme Trust for a senior Research fellowship for G S and Dr L M Reilly for useful discussions.

We are grateful for the contribution of Professor C N R Rao to this and many other areas in the field of solid-state chemistry. Many of us have benefited greatly from his unique qualities and his insatiable enthusiasm towards science.

References

1. Grasselli R K and Burrington J D 1981 *Adv. Catal.* **30** 133
2. MoroOka Y and Ueda W 1994 *Adv. Catal.* **40** 233
3. Theobald F, Laarif A and Hewat A W 1985 *Mater. Res. Bull.* **20** 653
4. Chen H and Sleight A W 1986 *J. Solid State Chem.* **63** 70
5. Teller R G, Brazdil J F and Grasselli R K 1984 *Acta Crystallogr.* **C40** 2001
6. Buttrey D J, Jefferson D A and Thomas J M 1986 *Philos. Mag.* **53** 897
7. Thomas J M and Thomas W J 1997 *Principles and practice of heterogeneous catalysts* (New York: VCH)
8. Aurivillius B 1951 *Ark. Kemi.* **2** 519
9. Antonio M R, Teller R G, Sandstrom D R, Mehicic M and Brazdil J F 1988 *J. Phys. Chem.* **92** 2939
10. Hearne G W and Adams M 1948 *US Patent* 2,451,485
11. Standard Oil Co 1964 *GB Patent* 965,173
12. McClellan W R and Stiles A B 1972 *US Patent* 3,678,139
13. Grasselli R K, Suresh D D and Friedrich M S 1984 *US Patent* 4,424,141
14. Sasaki Y, Mori K and Moriya K 1990 *EP Patent* 0,389,255
15. Sasaki Y, Mori K and Moriya K 1990 *EP Patent* 0,383,598
16. Kope J, Kripylo P, Hohlstamm I, Hoepfner R, Knaack K E and Mai H G 1993 *DE Patent* 4,124,666
17. Izumi J, Watanabe S and Yoshioka H 1997 *EP Patent* 0,799,642
18. Schirmann J P, Descat G, Etienne E, Pham C and Simon M 2000 *FR Patent* 278,251,2
19. Rao C N R and Gopalakrishnan J 1987 *Acc. Chem. Res.* **20** 228

20. Snyder T P and Hill C G 1991 *J. Catal.* **132** 536
21. Beale A M and Sankar G 2003 *Chem. Mater.* **15** 146
22. Sankar G, Wright P A, Natarajan S, Thomas J M, Greaves G N, Dent A J, Dobson B R, Ramsdale C A and Jones R H 1993 *J. Phys. Chem.* **97** 9550
23. Sankar G and Thomas J M 1999 *Topics Catal.* **8** 1–21
24. Reilly L M, Sankar G and Catlow C R A 1999 *J. Solid State Chem.* **148** 178
25. Beale A M and Sankar G 2002 *J. Mater. Chem.* **12** 3064
26. Depero L E and Sangaletti L 1995 *J. Solid State Chem.* **119** 428
27. Keulks G W, Hall J L, Daniel C and Suzuki K 1974 *J. Catal.* **34** 79
28. Bing Z, Pei S, Shishan S and Xiexian G 1990 *J. Chem. Soc., Faraday Trans.* **86** 3145